

DIAGNOSTICS OF DEFECT DETECTION IN THE INITIAL STAGES OF STRUCTURAL FAILURE USING THE ACOUSTIC EMISSION METHOD OF CONTROL

UDC: 620.179.16

Original scientific paper

<https://doi.org/10.18485/aeletters.2022.7.2.1>

Sergey Grazion¹, Valery Spiriyagin², Mikhail Erofeev³, Igor Kravchenko^{3,4}, Yury Kuznetsov^{*5}, Mikhail Mukomela⁶, Sergey Velichko⁷, Aleksandar Ašonja⁸, Larisa Kalashnikova⁹

¹ AO "Moscow Institute of Thermal Engineering Corporation", Moscow, Russia

² Moscow Aviation Institute (National Research University), Moscow, Russia

³ Institute of Mechanical Engineering of the Russian Academy of Sciences named after A.A. Blagonravov (IMASH RAS), Moscow, Russia

⁴ Russian State Agrarian University – MTA named after K.A. Timiryazev, Moscow, Russia

⁵ Orel State Agrarian University named after N.V. Parakhin, Orel, Russia

⁶ Peter the Great Military Academy of the Strategic Rocket Forces, Balashikha, Russia

⁷ National Research Mordovia State University named after N.P. Ogarev, Saransk, Russia

⁸ Faculty of Economics and Engineering Management in Novi Sad, University Business Academy in Novi Sad, Serbia

⁹ Orel State University named after I.S. Turgenev, Orel, Russia

Abstract:

The article presents the results of experimental estimation of the possibility of early registration of structural defects using the acoustic-emission method of control, based on the phenomenon of acoustic emission, which is the excitation of elastic vibrations of the material, caused by the formation and development of defects. To confirm the possibility of recording the processes of predestruction, such as the development of crack-like defects and plastic deformation using the acoustic-emission method of control, full-scale tests of the pressure vessel were carried out and the physical model of the shell-and-tube heat exchanger specially designed for this process was verified. It has been determined that the most informative frequency range for recording acoustic emission signals is the range of 100-200 kHz. The relationship of acoustic emission with the characteristics of defect development during plastic deformation has been studied. It was found that for reliable determination of the plastic deformation process, shared usage of amplitude and the count rate of acoustic emission is advisable.

ARTICLE HISTORY

Received: 06.04.2022.

Accepted: 12.06.2022.

Available: 30.06.2022.

KEYWORDS

Technical diagnostics,
Nondestructive testing,
Physical model, Shell and tube
heat exchanger

1. INTRODUCTION

Strength tests of items operating under load are carried out practically at all main stages of the life cycle, namely: at the stages of development and production - during acceptance tests, at the stages of operation - during technical certification and

service life extension. At that, the main criteria of technical condition estimation are the confirmation of durability and absence of deformation after the test.

The main disadvantage of strength tests is that loading the item to the test pressure P_{test} , higher than the operating pressure $P_{operating}$, can lead to the

*CONTACT: Y. Kuznetsov, e-mail: kentury@yandex.ru

formation of the crack-like defects or growth of the existing ones in the material. Since testing often does not use nondestructive testing methods to record these processes, the uncontrolled development of defects can lead to catastrophic consequences.

To investigate the possibility of reducing the impact of this disadvantage, items operating under the pressure were chosen as an example.

Uncontrolled formation of new defects or the growth of existing defects is especially dangerous for items made of high-strength metals, in which the critical length of the fracture defect $l_{critical}$ is less than the wall thickness.

Quantitative estimation of the influence of crack-like defects on the strength properties of materials is based on linear fracture mechanics [1-4].

Nowadays several criteria have been developed, which make it possible to estimate the resistance of materials and structural elements to cracking. The most developed and convenient from the engineering point of view is the stress intensity factor (SIF) [5-7]. The main advantage of the SIF is that, under a number of conditions, it can serve as a characteristic of the crack resistance of materials, just as tensile strength σ_t or yield strength $\sigma_{0.2}$ serve as strength characteristics. Thus, brittle fracture will occur if the active value of the SIF reaches the critical value of brittle fracture K_s (the minimum value of the SIF, at which the crack begins to spread avalanche-like at a speed comparable to the sound speed).

There are three shapes of local deformation at the crack apex: normal fracture (type I), transverse shear (type II) and longitudinal (pure) shear (type III). According to the shape of the deformation at the crack apex, the corresponding stress intensity factor (SIF) are distinguished: K_I , K_{II} , K_{III} . The most dangerous shape of deformation at the crack apex is the normal fracture, so the stress intensity factors are more often considered K_{II} .

A generalized expression for the actual stress intensity factor (SIF) is the following:

$$K_{II} = \pi \cdot \sigma \cdot \sqrt{l} \quad (1)$$

where K_{II} – active value of the SIF in case of the normal fracture;

σ – stresses in the item that do not take into account the presence of cracks;

l – crack length.

From expression (1) we can determine at what stress the crack growth will occur:

$$\sigma = \frac{K_{II}}{\pi\sqrt{l}} \quad (2)$$

If crack growth occurs during the strength test, then from formula (2) we can conclude that the stress at which crack growth occurs during subsequent loading will decrease.

In the future, when creating the operating load, the following variants of events are possible:

- ✓ the crack does not change its dimensions and the item retains its performance;
- ✓ the crack grows, reaching the value of l_{kp} , i.e. conditions for brittle fracture of the item are realized;
- ✓ the crack grows without reaching the value of l_{kp} , the item does not fail, but during exposure, under operating load or cyclic loading, it is possible to observe slow crack propagation up to the value of l_{kp} .

In order to level out this disadvantage, it is necessary to use nondestructive testing methods [8-11], which allow you to fix the fact of occurrence or defects development in the structure.

One of these methods is the method of acoustic emission (AE), based on the phenomenon of acoustic emission, which is the excitation of elastic vibrations of the material caused by the formation and development of defects [12-16]. These oscillations are recorded by receivers located on the structure surface. The location of the defect is determined by the sequence of arrival and time of registration of the elastic disturbance by several receivers. Other characteristics of the elastic disturbance, such as its amplitude, energy, duration and some other parameters, allow conclusions to be drawn about the nature of the detected defects [17, 18].

As a rule, acoustic-emission control is carried out during the testing of structures by loading, which is a stimulus for the manifestation of hidden defects [19-23]. At the same time, the acoustic-emission method also allows continuous control of objects, when the development of defects occurs under the influence of workloads and the environment. In this case, the conclusion about the state of the controlled object is given on the basis of the analysis of the AE process by identifying trends in its characteristics.

Compared to other methods of nondestructive testing, the AE method has the following advantages [12, 14-16]:

- ✓ allows you to isolate developing, i.e. the most dangerous defects, to detect developing defects long before the structure failure;
- ✓ to detect defects and determine their location in the entire volume of the material is sufficient to install some sensors on the construction surface;
- ✓ no personnel are required to be present in the close area of the structure when performing inspections;
- ✓ removal of thermal insulation (if any) is necessary only in places where sensors are installed;
- ✓ capable of detecting defects in structural areas that are inaccessible in principle for the use of other methods of nondestructive testing.

The main sources of AE in materials are: crack movement; development of the plastic zone at the crack apex; crack edge friction and destruction of corrosion products; stress corrosion and corrosion; delamination and destruction of inclusions; rupture of matrix elements and delamination in materials with a matrix structure.

AE is used both in the process of manufacturing items (control of phase transitions, welding control, etc.) and for the control of equipment during operation (periodic or continuous control). In addition to the main application acoustic emission is used to detect leaks and weakly fixed or free-moving objects.

To confirm the possibility of recording the processes of predestruction, such as the development of crack-like defects and plastic deformation using the acoustic-emission method of control, full-scale tests of the pressure vessel were carried out and the physical model specially developed for this process was tested.

The relevance of the research objects choice is conditioned by the safety of vessels and cylinders working under pressure and insufficient study of the acoustic-emission method.

2. MATERIALS AND METHODS

The test objects chosen were:

- 1) vessel cover (Fig. 1) to confirm the possibility of recording fracture-like defects;
- 2) a physical model of a shell-and-tube heat exchanger (SHE) to assess the possibility of recording plastic deformation.

The cover is made of cold-rolled sheet (GOST

19904-90/SP33-SH (Russia)) 2 mm thick. Mechanical material properties are: $\sigma_B = 165 \div 195$ kgf/mm²; $\delta \geq 7\%$. Welded joints are made by argon-arc welding with a non-consumable electrode using wire Св-20XCHBΦА TU 14-1-2683-79 (Russia). Before testing, the welded joints were subjected to radiation monitoring. No unacceptable defects were found. Then there were hydro-tests for strength with pressure 185 ± 4 kgf/cm² during 5 min and leak test by the method of "aquarium" pressure 10 ± 2 kgf/cm² during 5 min. After the strength and tightness tests, a magnetic particle testing according to GOST 21205-87 (Russia) was performed. According to the results of all tests no defects were detected.

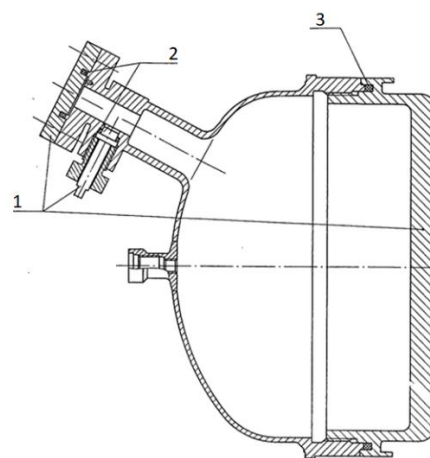


Fig. 1. Vessel cover

- 1 - technological plugs; 2 - technological gaskets;
3 - technological gasket

Then, loading of the cover to failure was carried out. The loading was performed in an armor chamber with high-speed video recording of the loading and fracture process, and control using the AE method.

A high-speed camera with a shooting speed of 5000 frames per second was used for video recording. To control the parameters of acoustic emission signals, the Malakhit AS-14A AE system was used to detect and record AE sources, measure the parameters of AE signals to monitor the condition of potentially hazardous equipment.

Any item is a kind of waveguide for acoustic waves arising from acts of destruction. The characteristics of acoustic waves in the product depend on many factors such as - material, wall thickness, design features, etc. Therefore, to determine the most informative frequency range of control, two acoustic emission receivers (AER) were installed on the item: DR15I with a resonance frequency of 150 kHz and DR6I with a resonance

frequency of 60 kHz. According to GOST R 52777-2007 and GOST R 55045-2012 the total count, amplitude and number of signals were chosen as the main informative parameters of AE signals.

The second test object was a physical model of shell-and-tube heat exchanger (SHE) (Fig. 2), which was: the body 1 in the form of a cylinder with diameter 170 mm and wall thickness 9 mm, made of steel *Cm3cn4* with flat covers 2 and 3, welded to the body 1 on its ends, and made of the same material; the test object in the form of a test pipeline 4, made of copper grade *M3p*, diameter 20 mm and wall thickness 2 mm, rolled from two ends in the bush 5 with external thread and installed in the inner cavity of the body 1.

To initiate the process of plastic deformation, the test pipeline 4 was made with a pre-applied defect 6 in the form of an elliptical deflection. An example of the shape and location of the deflection is shown in Fig. 3.

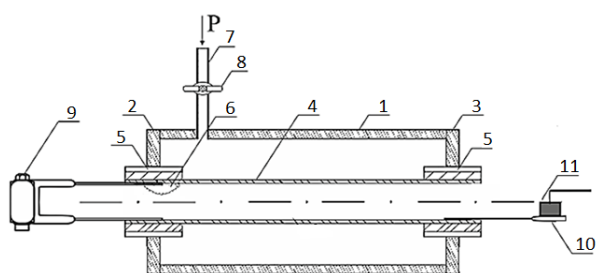


Fig. 2. Physical model of shell-and-tube heat exchanger

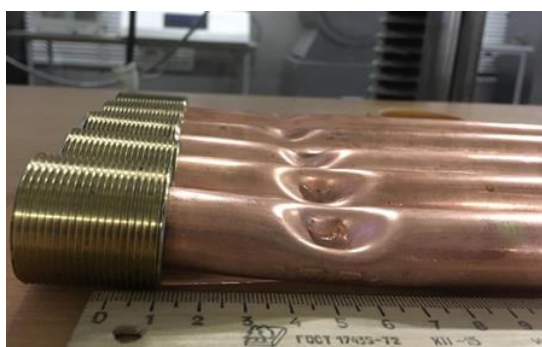


Fig. 3. Test pipelines with elliptical defects in the form of an elliptical deflection

The pipe deformation was controlled by the UB-5A displacement sensor 9, made in the form of a bracket. In order to record the AE signals, acoustic emission receiver (AER) GT200 11 was mounted on the acoustic via waveguide 10, made in the form of a plate of copper *M3p* and soldered to the test pipeline. Acoustic emission receiver (AER) is connected to the data reception and processing equipment, made in the form of an analog-digital A-

Line32D unit (Interunis LLC., Moscow). Sensor 9 recorded the tube movement caused by plastic deformation, and sensors 10 recorded the AE signals generated in this process.

Based on the results of [24-26], the average amplitude and AE count rate were chosen as the most informative AE parameters indicating the development of plastic deformation.

3. RESULTS AND DISCUSSION

To analyze the processes occurring during lid loading, a linear style of graphs was used (column-sum (the data falling in the column are summed)). In contrast to the maximum and average amplitudes and signals, these indicators are integral. Graphs of total count for all loading time (Fig. 4 and 5), as well as total amplitude (Fig. 6 and 7) and total signals (Fig. 8 and 9) allow us to conclude that the total count, total amplitude and number of AE signals recorded by DR15I are twice as high as those recorded by DR6I. Thus, the most informative frequency range is the 100-200 kHz range, i.e., the results of registration of AE signal parameters using the DR15I will be used for further analysis. Generalized graphs of the total amplitude, total number of signals per unit time recorded by the DR15I and the voltage in the item material are shown in Fig. 10.

After analyzing the graphs, it can be noted that the dynamics of changes in the signal parameters does not differ from similar ones for most defect-free metals. Three characteristic areas can be distinguished:

- ✓ when loaded up to $\sigma \sim 50 \text{ kgf/cm}^2$ is characterized by high emission activity of AE signals, which is explained by metal stretching during loading and triggering of AE signal sources, most optimally oriented to the applied load;
- ✓ when loading up to $\sigma \sim 50-145 \text{ kgf/cm}^2$ low activity of AE signal emission is explained by the fact that the main AE sources have triggered, material hardening occurred and micro-destruction processes take place (dislocation movement and/or merging, etc.) which have low energy and most of them simply cannot be registered by the equipment;
- ✓ when loading $\sigma > 145 \text{ kgf/cm}^2$ a sharp increase in activity, which is explained by the development of pre-fracture processes (micro-defects merge into macro-defects, macro-defects grow up).

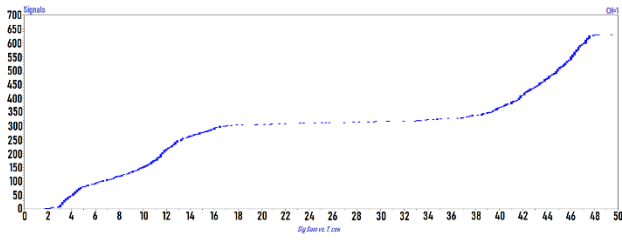


Fig. 4. Total count of AE signals for the whole test time, recorded by the acoustic emission receiver AER DR151

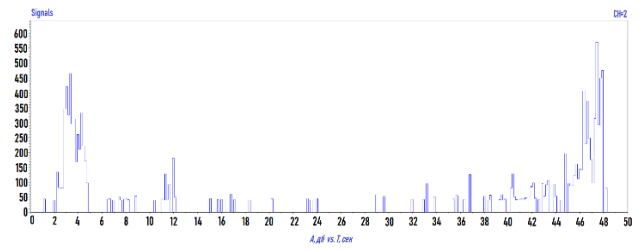


Fig. 9. Total amplitude of AE signals recorded by the DR61 per time unit

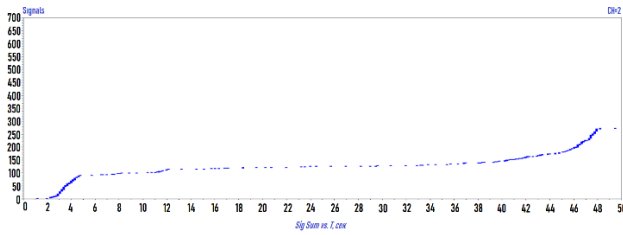


Fig. 5. Total count of AE signals for the whole test time, recorded by the acoustic emission receiver AER DR61

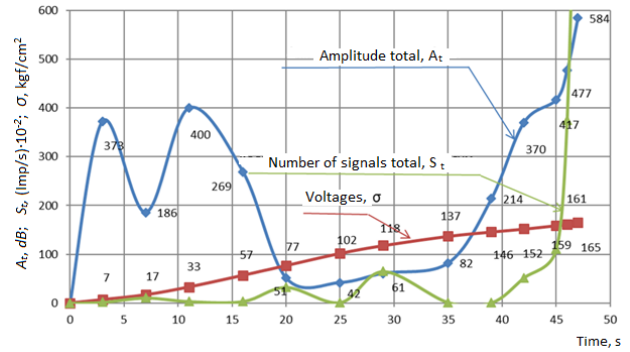


Fig. 10. Generalized graphs of total amplitude, total number of signals per unit time, recorded by DR151 and voltage in the item material

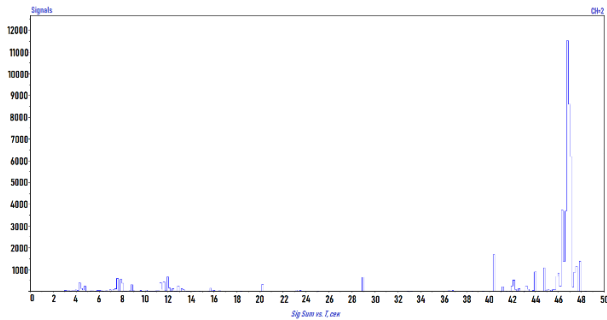


Fig. 6. Total number of signals recorded by the DR151 per time unit

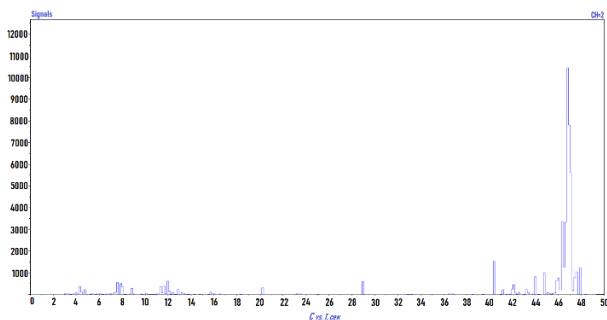


Fig. 7. Total number of AE signals recorded by DR61 per time unit

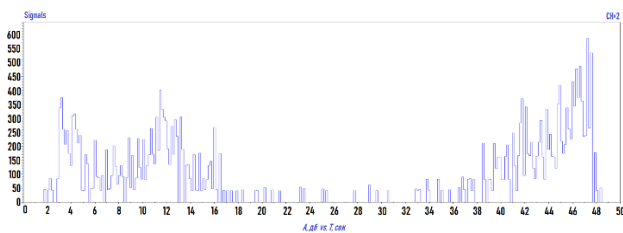


Fig. 8. Total amplitude of AE signals recorded by DR151 per time unit

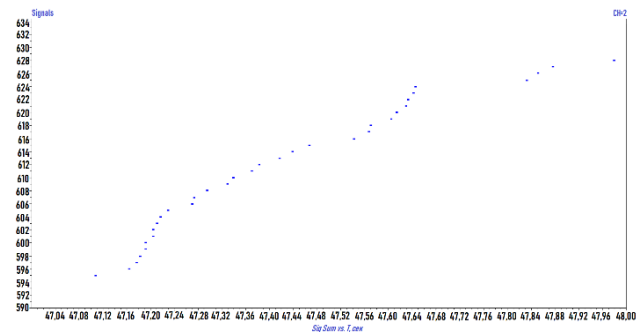


Fig. 11. Graph of the total count of AE signals at 47 s

For a more detailed analysis of the predestruction process, let us consider the time range from 45 to 47 sec. Fig. 12 and 13 show graphs of the total amplitude and total number of AE signals.

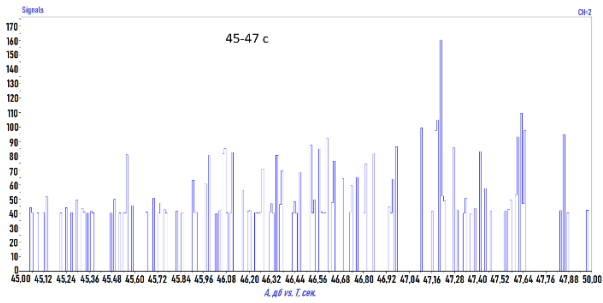


Fig. 12. Total amplitude graph

The results of the analysis of Fig. 12 show that starting from 45.55 sec individual bursts of radiation with an amplitude of 80 dB and higher are recorded. The recorded signals between the bursts are explained by the processes of microfracture, leading to the accumulation of microdefects, and the bursts by the merging of microdefects into macrodefects. At the same time, the maximum total amplitude is recorded at 47.25 s, which is probably associated with the formation of the main crack, and at 47.64 s with its opening.

The graph of the total number of AE signals also shows bursts (Fig. 13). Bursts with a value greater than 689 begin to be registered from 45.90 sec and reach their maximum at 46.98 sec.

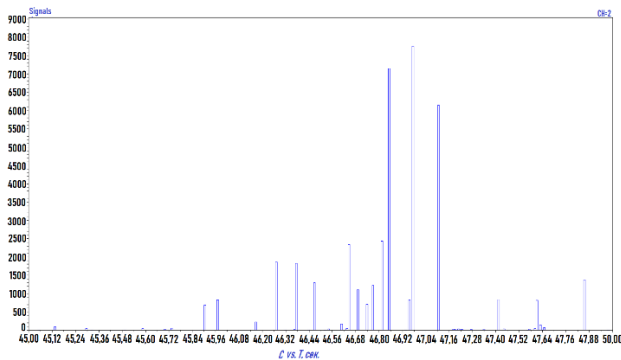


Fig. 13. Graph of the total number of signals

Considering the generalized graphs (Fig. 14), it can be noted that in time the bursts of the total number of signals are ahead of the bursts of the total amplitude of the recorded AE signals. This is explained by the fact that initially there is an accumulation process of microdefects, deformation in the crack apex, which is accompanied by a large number of low-amplitude AE signals. After the critical number of microdefects is reached, they

merge with the formation of macrodefects, and when the critical size of the deformation zone at the crack apex is reached, a jump-like growth of the crack occurs, and both processes are accompanied by a smaller number of AE signals, but with a high amplitude. After manufacturing the body of the shell-and-tube heat exchanger (SHE) model and installing the test pipeline containing the defect, the physical model was placed in an armored chamber with the possibility of supplying AE transducers and the pipeline from the pumping station. Then, the hydrostatic test pressure was stepwise increased in steps of 0.1 MPa, after which the test pipeline was exposed and the AE signals were recorded.

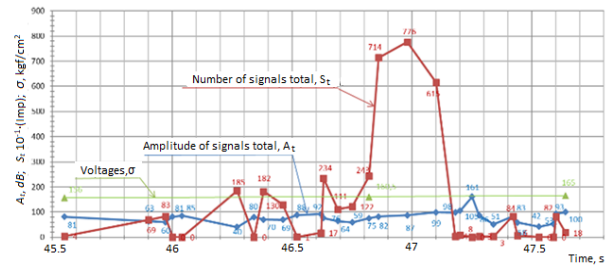


Fig. 14. Plots of AE signal parameters and voltage in the cover material

The test was stopped after receiving signals from strain gauge about pipe deformation, recording average AE amplitude (u_m) signals above discrimination threshold (39 dB) and simultaneous increase of AE count rate (\dot{N}), accompanying plastic deformation when the yield stress of the material is reached (Fig. 15).

When creating hydrostatic pressure in the intertube space, static exposure under overpressure was performed for 30 seconds in increments of 0.8 MPa.

In the course of tests at the loading stage a continuous AE with amplitude up to 50 dB associated with turbulent motion of liquid was observed. At the exposure stages the AE parameters, not related to the fluid motion and the presence of which indicates the degradation processes of the material, were monitored. As it can be seen from Fig. 15, no AE signals were detected at the exposure stages at pressures of 0.8 MPa (90-120 s) and 1.6 MPa (190-220 s).

When the test pressure was increased to 2/3 MPa, signals from the displacement sensor and a simultaneous increase in the AE count rate were recorded, which indicated the beginning of the degradation process. At the stage of exposure under test pressure of 2.4 MPa (300-320 s), the recording of AE signals with an average amplitude

above the discrimination threshold (up to 58 dB) and an increase in the AE count rate (region 1 in Fig. 15a and b) was continued.

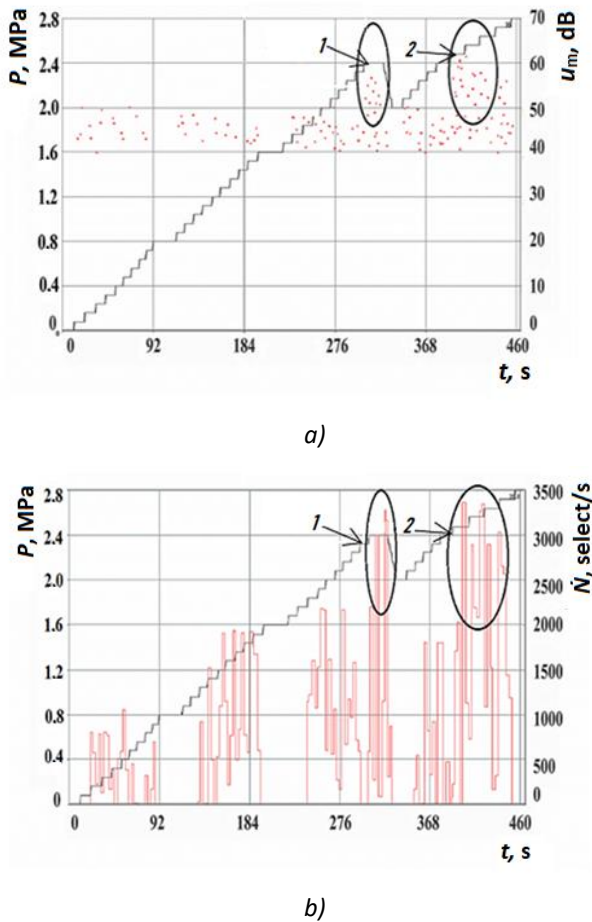


Fig. 15. Graphical representation of AE signals during hydraulic loading of a test pipeline with a defect: a - average amplitude; b - AE count rate

For accurate interpretation of the AE signal source and elimination of false signals associated with possible leaks, the test pressure was reset to 2 MPa and reloaded above the previous load level. Before reaching the pressure of 2.4 MPa, the AE corresponding to the level of turbulent fluid motion was observed. At exceeding the test pressure, due to the Kaiser effect [27], at the time interval of 395-440 sec (region 2 in Fig. 15a and b) a further increase in the average amplitude and AE count rate was observed. It provides accurate interpretation of the received signals as acoustic emission of plastic deformation of the heat exchange tube.

The proposed control method can be applied to develop programs and methods of inspection and increase the service life of shell-and-tube heat exchangers, regardless of their geometric and mass-size characteristics.

4. CONCLUSION

The following conclusions were made on the basis of the research conducted:

- ✓ All processes occurring in the item material during loading are accompanied by acoustic emission. The most informative frequency range for recording AE signals is the range of 100-200 kHz. Test loading with AE control will allow avoiding uncontrolled nucleation and development of defects in the structure;
- ✓ Analysis of the parameters of AE signals when loading a defect-free product allows predicting failure at 90-93% of the destructive load;
- ✓ The choice of loading scheme (loading rate, constant loading or with exposures, pressure value and duration of exposures at exposures steps) will avoid failure in a guaranteed manner;
- ✓ To recognize the type of defect (plastic deformation, crack development, etc.) it is necessary to load samples (with and without defect), made of the item material with AE control, to their fracture;
- ✓ The peculiarity of AE signals during plastic deformation is the generation of a large number of pulses of low amplitude and energy, due to which the detection of a useful signal against the background of external noise can be difficult. For reliable determination of the plastic deformation process, it is reasonable to use the joint use of AE amplitude and count rate.

REFERENCES

- [1] C. E. Seow, Ji. Zhang, H. E. Coules, G. Wu, C. Jones, Ji. Ding, S. Williams, Effect of crack-like defects on the fracture behaviour of Wire + Arc additively manufactured nickel-base alloy 718. *Additive Manufacturing*, 36 (12), 2020: 101578. <https://doi.org/10.1016/j.addma.2020.101578>
- [2] M. Marco, D. Infante-Garcia, R. Belda, E. Giner, A comparison between some fracture modelling approaches in 2D LFM using finite elements. *International Journal of Fracture*, 223 (1-2), 2020: 151-171. <https://doi.org/10.1007/s10704-020-00426-6>
- [3] S.A. Sedmak, Computational fracture mechanics: An overview from early efforts to recent achievements. *Fatigue & Fracture of*

- Engineering Materials & Structures*, 41 (12), 2018: 2438-2474.
<https://doi.org/10.1111/ffe.12712>
- [4] C.V. Doronin, A.M. Lepikhin, V.V. Moskvichev, Y. I. Shokhin, A.M. Lepikhin, V.V. Moskvichev, Modeling of Strength and Failure of Supporting Structures of Technical Systems: Strength, Fracture Mechanics, Resource, Safety of Technical Systems, ed. Nauka. Siberian Publishing Company. Novosibirsk, 2005.
- [5] K.A. Molokov, V.V. Novikov, Evaluation of crack resistance of welded joints with soft interlayers. *Advanced Engineering Research*, 21 (4), 2021: 308-318.
<https://doi.org/10.23947/2687-1653-2021-21-4-308-318>
- [6] D. Peng, C. Wallbrink, R. Jones, An assessment of stress intensity factors for surface flaws in a tubular member. *Engineering Fracture Mechanics*, 72 (3), 2005: 357-371.
<https://doi.org/10.1016/j.engfracmech.2004.04.001>
- [7] C.A. Sokolov, D.E. Tulin, A Method of Calculation of Stress Intensity Coefficient for a Crack in the Stress Concentrator Area. Proceedings of Tula State University. Technical Sciences, 5, 2020: 328-335.
- [8] S. Gholizadeh, A review of non-destructive testing methods of composite materials. *Procedia Structural Integrity*, 1, 2016: 50-57.
<https://doi.org/10.1016/j.prostr.2016.02.008>
- [9] V.V. Nosov, A.I. Potapov, Acoustic-emission testing of the strength of metal structures under complex loading. *Russian Journal of Nondestructive Testing*, 51 (1), 2015: 50-58.
<https://doi.org/10.1134/S1061830915010064>
- [10] F. BJORHEIM, S. C. SIRIWARDANE, D. PAVLOU, A review of fatigue damage detection and measurement techniques. *International Journal of Fatigue*. 154, 2022: 106556.
<https://doi.org/10.1016/j.ijfatigue.2021.106556>
- [11] M.M. Kuten, A.L. Bobrov, Development of a technique for identifying dangerous defects in objects subjected to acoustic-emission control. The Siberian transport university bulletin, 4 (59), 2021: 62-68.
- [12] T.M. Roberts, M. Talebzadeh, Acoustic emission monitoring of fatigue crack propagation. *Journal of Constructional Steel Research*, 59 (6), 2003: 695-712.
[https://doi.org/10.1016/S0143974X\(02\)00064-0](https://doi.org/10.1016/S0143974X(02)00064-0)
- [13] E. Agletdinov, E. Pomponi, D. Merson, A. Vinogradov, A novel Bayesian approach to acoustic emission data analysis. *Ultrasonics*, 72 (12), 2016: 89-94.
<https://doi.org/10.1016/j.ultras.2016.07.014>
- [14] T. Shiraiwa, K. Ishikawa, M. Enoki, I. Shinozaki, S. Kanazawa, Acoustic emission analysis using Bayesian model selection for damage characterization in ceramic matrix composites. *Journal of the European Ceramic Society*, 40 (8), 2791-2800.
<https://doi.org/10.1016/j.jeurceramsoc.2020.03.035>
- [15] Z. Su, Ch. Zhou, M. Hong, Li Cheng, Q. Wang, X. Qing, Acousto-ultrasonics-based fatigue damage characterization: Linear versus nonlinear signal features. *Mechanical Systems and Signal Processing*, 45 (1), 2014: 225-239.
<https://doi.org/10.1016/j.ymsp.2013.10.017>
- [16] H.A. Semashko, V.I. Shport, B.N. Mar'in, Acoustic Emission in Experimental Materials Science, ed. Mechanical Engineering, Moscow, 2002.
- [17] Z. Nazarchuk, O. Andreykiv, V. Skalskyi, D. Rudavskyi, Acoustic emission method in the delayed fracture mechanics of structural materials. *Procedia Structural Integrity*, 16, 2019: 169-175.
<https://doi.org/10.1016/j.prostr.2019.07.037>
- [18] M.G. Droubi, N.H. Faisal, F. Orr, J.A. Steel, M.N. El-Shaib, Acoustic emission method for defect detection and identification in carbon steel welded joints. *Journal of Constructional Steel Research*, 134 (7), 2017: 28-37.
<https://doi.org/10.1016/j.jcsr.2017.03.012>
- [19] V.V. Nosov, On the principles of optimizing the technologies of acoustic-emission strength control of industrial objects. *Russian Journal of Nondestructive Testing*, 52 (9), 2016: 386-399.
<https://doi.org/10.1134/S106183091607006>
- [20] O. Stankevych, Valentyn Skalsky, Investigation and identification of fracture types of structural materials by means of acoustic emission analysis. *Engineering Fracture Mechanics*, 164, 2016: 24-34.
<https://doi.org/10.1016/j.engfracmech.2016.08.005>
- [21] A. Rai, Z. Ahmad, M.J. Hasan, J.-M. Kim, A novel pipeline leak detection technique based on acoustic emission features and two-sample Kolmogorov-Smirnov test. *Sensors*, 21 (24), 2021, 8247.
<https://doi.org/10.3390/s21248247>

- [22] A.V. Sokolkin, I.Y. Ievlev, S.O. Cholakh, Methods to testing bottoms of tanks for oil and oil derivatives. *Russian Journal of Nondestructive Testing*, 38, 2002: 113-115. <https://doi.org/10.1023/A:1020546307628>
- [23] A. N. Kuzmin, A.B. Zhukov, D.G. Davydova, D.V. Shchitov, E.G. Akselrod, V.A. Kats, Acoustic-emission control in assessing the technical condition of oil and gas complex equipment. *In the World of Nondestructive Testing*, 20 (1), 2017: 71-80.
- [24] B.V. Spiryagin, I.A. Medelyaev, A.I. Chmykhalo, Model of loss of serviceability of metal structures of a refrigeration machine evaporator. *Assembling in Mechanical Engineering, Instrumentation*, 11, 2019: 483-492.
- [25] A. Vinogradov, A.V. Danyuk, D.L. Merson, I.S. Yasnikov, Probing elementary dislocation mechanisms of local plastic deformation by the advanced acoustic emission technique. *Scripta Materialia*, 151, 2018: 53-56. <https://doi.org/10.1016/j.scriptamat.2018.03.036>
- [26] V. Marasanov, A. Sharko, Mathematical models for interrelation of characteristics of the developing defects with the parameters of acoustic emission signals. *International Frontier Science Letters*, 10, 2016: 37-44, 2016. <https://doi.org/10.18052/www.scipress.com/IFSL.10.37>
- [27] I.A. Medelyaev, V.V. Spiryagin, A.I. Chmykhalo, Experimental Assessment of the Effect of Imperfect Geometric Form of Heat Exchange Tubes on the Value of Critical Pressure. *Assembling in Mechanical Engineering, Instrumentation*, 12, 2019: 531-536